REPEATABLE EXPLOSIVE-DRIVEN PULSE GENERATOR SYSTEM

R. L. Schlicher, D. J. Hall

Air Force Weapons Laboratory
Kirtland AFB, NM 87117

ABSTRACT

A device is described which generates electrical pulses from low explosives without selfdestructing. The device incorporates an explosive propellant actuator coupled to an explosive propellant driver which drives a rare-earth permanent magnet linear generator to generate the electric pulse. A mechanical pneumatic-spring mechanism provides a method of system recovery and reset. Although the proof-of-principle laboratory device generates pulses in the milliwatt range (using a .22 caliber Hornet case), the technology it represents may be scalable to produce peak power pulses above a megawatt. The results of a series of live test firings conducted in the fall of 1986 and into the spring of 1987 are discussed in some detail.

1. Introduction

In this paper, we outline the design and method of the Repeatable Explosive-Driven Pulse Generator System. The laboratory proof-of-principle device includes an explosive propellant actuator which couples to an explosive propellant driver which then drives a rare-earth permanent magnet linear generator to generate the electric pulse. A mechanical pneumatic-spring mechanism provides a method of system recovery and reset. Test firings were conducted at the AF Weapons Laboratory to determine system behavior so that its performance could be modeled for future feasiblity studies. On June 10, 1986, patent 4,594,521 was issued for this generator system.[1]

2. General Design Concept Development

This particular pulsed power generator system resulted from an effort to determine the feasibility of repetitive explosive-driven generators for pulsed high power aerospace applications. Both high (detonating) and low (propellant) explosive actuation methods were analyzed for use in repetitive devices. A study of High Explosive (HE) driven pulsed generators indicated the need for materials with tensile and sheer strengths in excess of 1 million psi to achieve repeatability.[2] Consequently, the effort focused on explosive propellant driven pulsed generators.

The concept of explosive propellant driven generators is not new. Shortly after World War II, C. B. Gardner conducted a series of tests in which an aluminum cylindrical slug was propelled down a smooth bore tube into an axial magnetic field generated by an external coil mounted midway down the tube.[3] The slug passed through the axial center of the tube and was allowed to exit the tube to a undetermined destination. Explosively moving a permanent magnet in and out of a magnetic circuit was also studied. Unfortunately, high coercivity magnets did not exist at that time and the magnets degaussed or reversed polarity during an single cycle.

During the 1960s, S. D. Weisman, et al developed a device that was mounted at the end of an infantry rifle.[4] Cylindrical aluminum bullets were fired through the device's internally mounted solenoid coil which was aligned axially with the rifle barrel.

An initial magnetic field was provided externally. The passage of the aluminum bullet through the solenoid suddenly changed its reluctance causing a high voltage pulse at the solenoid terminals. Serious work in this area ceased until the early 1980s when rare earth permanent magnets were readily available and inexpensive.

For the study of repetitive explosive propellant driven permanent magnet generators, rare earth samarium-cobalt magnets were selected as the magnetomotive (MMF) source because of their high energy product (approximately 20 megaoersteds) and exceptionally high coercivity. The permanent magnet is propelled out of the magnetic flux circuit by a mechanically attached piston placed in the smooth bore barrel. The technology embodied in pnuedraulic mechanisms used to recover artillery rifles after firing was incorporated into the recovery and reset mechanism of the generator system. Finally, an electric driven solenoid-actuated hammer was invented to provide the necessary percussion for the primer on the center-fire cartridges.

3. The Generator System

The repeatable explosive-driven pulse generator system (see figure 1) consists of four distinct subsystems: 1) explosive actuator, 2) explosive propellant driver, 3) permanent magnet linear generator, and 4) braking and recovery mechanism. Figure 2 is drawing of an artist concept for implementing the generator system.
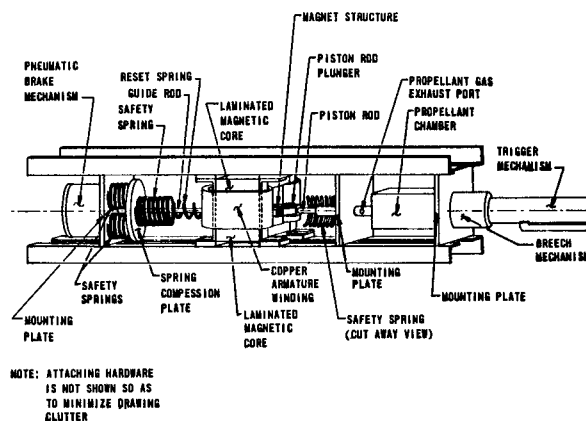

Fig. 1. Generator System Block Diagram.

Fig. 2. Conceptual Drawing of Generator System.

430

Report Documentation Page		*Form Approved* *OMB No. 0704-0188*

1. REPORT DATE **JUN 1987**	2. REPORT TYPE **N/A**	3. DATES COVERED **-**
4. TITLE AND SUBTITLE **Repeatable Explosive-Driven Pulse Generator System**		5a. CONTRACT NUMBER
		5b. GRANT NUMBER
		5c. PROGRAM ELEMENT NUMBER
6. AUTHOR(S)		5d. PROJECT NUMBER
		5e. TASK NUMBER
		5f. WORK UNIT NUMBER
7. PERFORMING ORGANIZATION NAME(S) AND ADDRESS(ES) **Air Force Weapons Laboratory Kirtland AFB, NM 87117**		8. PERFORMING ORGANIZATION REPORT NUMBER
9. SPONSORING/MONITORING AGENCY NAME(S) AND ADDRESS(ES)		10. SPONSOR/MONITOR'S ACRONYM(S)
		11. SPONSOR/MONITOR'S REPORT NUMBER(S)

12. DISTRIBUTION/AVAILABILITY STATEMENT
Approved for public release, distribution unlimited

13. SUPPLEMENTARY NOTES
See also ADM002371. 2013 IEEE Pulsed Power Conference, Digest of Technical Papers 1976-2013, and Abstracts of the 2013 IEEE International Conference on Plasma Science. Held in San Francisco, CA on 16-21 June 2013. U.S. Government or Federal Purpose Rights License

14. ABSTRACT

A device is described which generates electrical pulses from low explosives without selfdestructing. The device incorporates an explosive propellant actuator coupled to an explosive propellant driver which drives a rare-earth permanent magnet linear generator to generate the electric pulse. A mechanical pneumatic-spring mechanism provides a method of system recovery and reset. Although the proof-of-principle laboratory device generates p~lses in the milliwatt range (using a .22 caliber Hornet case), the technology it represents may be scalable to produce peak power pulses above a megawatt. The results of a series of live test firings conducted in the fall of 1986 and into the spring of 1987 are discussed in some detail.

15. SUBJECT TERMS					

16. SECURITY CLASSIFICATION OF:			17. LIMITATION OF ABSTRACT	18. NUMBER OF PAGES	19a. NAME OF RESPONSIBLE PERSON
a. REPORT **unclassified**	b. ABSTRACT **unclassified**	c. THIS PAGE **unclassified**	**SAR**	**8**	

In the explosive actuator, electric solenoids propel a hammer against the firing pin of the explosive propellant driver. The explosive propellant driver then rapidly generates high pressure gas which expands adiabatically against a piston at the generator end of the gas expansion chamber. With a proper electrical load matched to a explosive propellant load, a maximum of 14 percent of the total available chemical energy can be converted into an electrical pulse of a millisec or more duration. An external simplified pulse forming network could then compress the pulsed power output to match the requirements of a specific load.

The gas expansion chamber serves as a gas pressure moderator to prevent chamber overpressure and to control the combustion process. Without an electrical load, the mechanical pneudaulic-spring mechanism must absorb and dissipate all the energy from the expanding gas. Vent ports at the end of the expansion chamber provide residue pressure relief upon full extension of the generator slidor stroke, thereby allowing system reset.

Pulse shape and duration is determined by generator geometry, total electric circuit impedance, explosive combustion characteristics, the permeability of the linear generator's magnetic flux circuit, and the performance characteristics of the permanent magnet. To prevent degaussing of the permanent magnet, the generator slidor begins its pulse cycle inserted into the magnetic flux circuit. The pole faces of the slidor are perpendicular to its direction of motion and aligned with the flux path of the magnetic circuit. Upon initiation, the explosive driver rapidly drives the slidor out of the magnetic flux ciruit. The Electromotive Force (EMF) induced by Lenz's and Faraday's Laws at the generator stator output terminals is such as to restrain the slidor in the flux circuit. With the proper electrical load, the slidor has minimal displacement as up to 96 percent of the available kinetic energy is converted into electrical pulse energy.

4. Thermodynamic Analysis[5]

Since the chemical reaction with its resultant heat and high pressure gas release is complete within milliseconds, we have assumed a thermodynamic adiabatic process occurs. Figure 3 illustrates the dimensions of the expansion chamber in front of the propellant charge. Table 1 is a list of the variables used to determine the work done by the high pressure gas in moving the generator slidor.
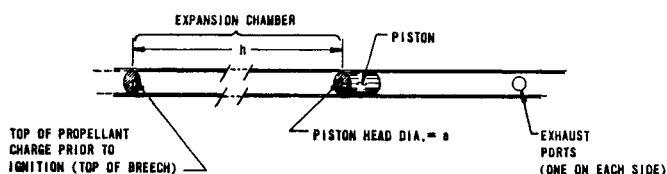

Fig. 3. Expansion Chamber

Table 1

Expansion Chamber Parameters

P_1 = Initial Pressure
V_1 = Initial Volume
P_2 = Subsequent Pressure
V_2 = Subsequent Volume
$\#$ = Ratio of the heat capacity = C_p/C_v

a = area of the top of the piston head

h = initial length of the expansion chamber

The thermodynamic cycle of the generator system is assumed to be the following:

    i. A predetermined propellant charge is loaded in the breech.
    ii. The piston is positioned a distance "h" from the top of the breech or the propellant charge.
    iii. The propellant charge is ignited.
    iv. The gas generated by the propellant charge rapidly fills the expansion chamber and raises its ambient pressure up to the initial operating pressure. For a slow burning propellant, the pressure will be approximately constant during a small initial volume displacement.
    v. With the expansion chamber rapidly pressurized, the working gas then expands against the piston-slidor assembly, doing work until the top of the piston passes the exhaust ports.
    vi. As the piston passes the exhaust ports, the remaining chamber pressure rapidly drops to atmospheric pressure.
    vii. The piston-slidor assembly is reset with the piston at the initial distance "h". The cycle repeats itself for automatic multiple shots.

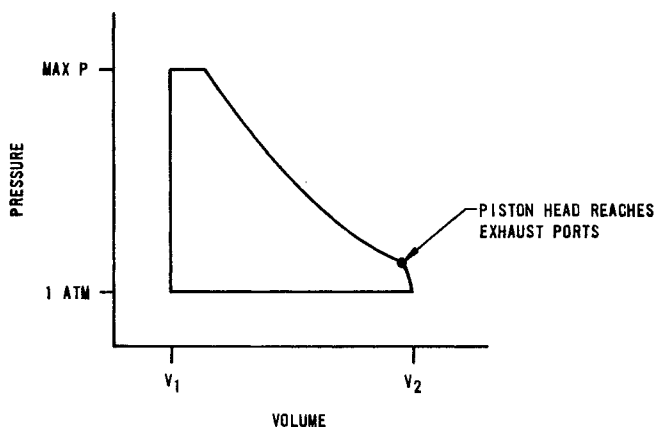Figure 4 illustrates this thermodynamic cycle which appears to approximate the ideal rankine cycle.

Fig. 4. Thermodynamic Cycle

For an adiabatic expansion we have the following expression for the work done by the expanding gas.

$$W = (P2V2 - P1V1)/\{1 - \#\}$$

Since the energy of the chemically released high pressure gas is initially converted into the kinetic energy of the piston-slidor assembly mass "M"

$$Mu^2/2 = (P_2V_2 - P_1V_1)/\{1 - \#\}$$

Where M = piston-slidor assembly mass
      u = piston-slidor assembly velocity.

Note that for any two points in an adiabatic process

$$P_1V_1^\# = P_2V_2^\#$$

and assuming that P_1 and V_1 are the initial conditions at the start of the device, then

$$P_1V_1^\# = C \text{ (a constant), or}$$

$$P_1 = C/\{V_1^\#\} \text{ and } P_2 = C/\{V_2^\#\}.$$

431

Substituting for P_1 and P_2 into the work function we have

$$Mu^2/2 = \{C[V_2^{1-\#} - V_1^{1-\#}]\}/(1-\#).$$

Setting x = distance traveled by the piston from its initial conditions, the work function becomes

$$Mu^2/2 = C\{\{[a(h+x)]^{1-\#} - [ah]^{1-\#}\}/(1-\#)\}$$

which is also an expression for the kinetic energy from the working gas. From this we can derive a velocity function

$$u(x) = SQR\{\{2C/M(1-\#)\}\{[a(h+x)]^{1-\#} - [ah]^{1-\#}\}\}.$$

The foregoing is analysis for first order thermodynamic adiabatic effects. We assumed that the working gas instantaneously goes from atmospheric pressure to the full initial working pressure. Furthermore, we assumed that the gas mixture was 80 percent nitrogen and it behaved ideally. For nitrogen the ratio of the heat capacities, $\# = 1.40$.

Since a minimum of 86 percent of the released chemical energy results in waste heat, cooling becomes a problem to the designer. Venting the exhaust gasses does help but for automatic cartridge fed generator systems an active cooling system is necessary to maintain the breech and expansion chamber materials within a safe temperature range.

5. Electromechanical Analysis[6]

This section describes analysis that predicts the output voltage and current along with the mechanical forces between the slidor and the stator. Only first order effects are considered. Fringing field effects are ignored. We also assume that the permanent magnet in the slidor behaves as a constant MMF source.[7] Only resistive loads are considered and analyzed. Again, ideal materials and conditions are assumed.
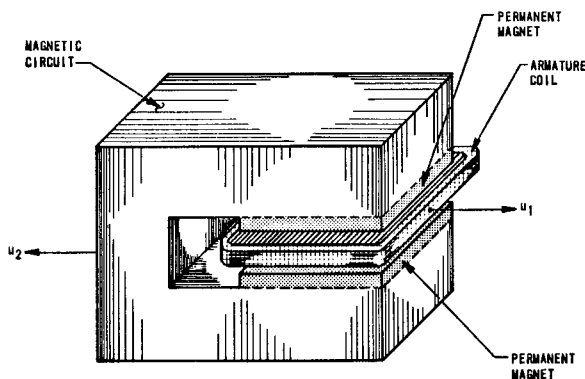

Fig. 5. Simple Linear Generator Model

Where a conductor coil perpendicular into a magnet field and the magnetic field are both moving in opposite directions at constant velocities (see figure 5), we have the following expression for the EMF induced at the output terminals of the coil.

$$EMF_s = \sum_{i=1}^{n} [1 + 2(i-1)s](u_1 + u_2)$$

Where l = Length of conductor perpendicular to direction of motion
s = Separation between subsequent loops in

the same plane
u_1 = Velocity of the stator coil relative to the center of mass of the slidor-stator system
u_2 = Velocity of the magnet field and hence the slidor relative to the center of mass of the slidor-stator system
B = Magnitude of the flux density bounded by the conductor loops
n = Number of stator coil loops or turns.

The foregoing expression assumes that the conductor loops are rectilinear in form and that each loop is connected in series with the preceding loop (see figure 6).
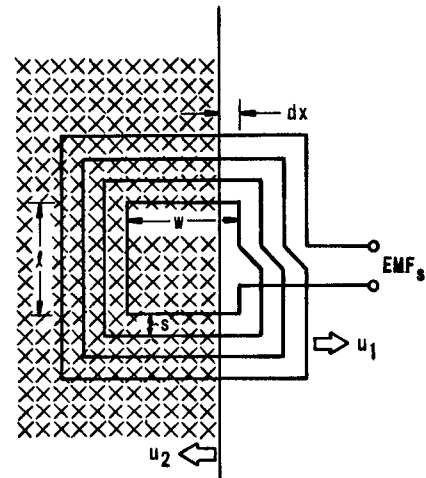

Fig. 6. Series Wound Coil Diagram.

Assuming that the separation distance "s" is negligible, that $u_1 = 0$ for the stator, and that stacking planes of conductor loops, all connected in series, add linearly to the net output voltage, we have the following simplification.

$$EMF_s = nlBu_2$$

where u_2 is now the velocity relative to the initial rest position of the center of mass of the slidor.

For the EMF due to the changing current and self-inductance of the stator coils, we have the following general expression:

$$EMF_a = -L(dI/dt)$$

Where L = Stator Self-inductance
I = Stator Coil Current

For a constant velocity u_2, we have the following formula for current, I:

$$I = EMF_s/R$$

Where R = Stator Net resistance plus external load.

So $I = nlBu_2/R$

and $dI/dt = \{nlB/R\}(du_2/dt)$

thus $EMF_a = +/- \{nlBL/R\}(du_2/dt).$

The +/- sign depends whether the slidor is accelerating or decelerating. Acceleration of the slidor causes a change in the net stator coil current

and the induced EMF_a is such as to oppose the direction of the change. This induced EMF_a is additive to the steady state EMF_s.

From experience, we propose the linear generator's motion can be broken up into four phases: Phase I, initial acceleration of the slidor; Phase II, constant velocity of the slidor; Phase III, deceleration of the slidor; and Phase IV, reset the slidor to the start position.

For Phase I we have the following:

$$EMF_i = nlBu_2 - \{nlBL/R\}(du_2/dt)$$

where the second term is negative since the current is increasing from zero.

For Phase II we have the following:

$$EMF_{ii} = nlBu_2$$

For Phase III we have the following:

$$EMF_{iii} = nlBu_2 + \{nlBL/R\}(du_2/dt)$$

where the second term is positive because the curent is decreasing.

For Phase IV, if the load is not disconnected after the initial pulse and the reset mechanism rapidly returns the slidor to its start position, a pulse of smaller amplitude but with the same general shape may be observed.
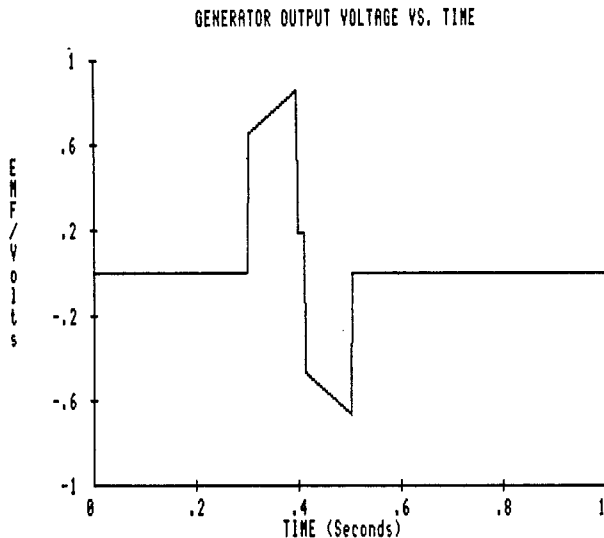

Fig. 7. Voltage Vs. Time Plot (1st order approx.).

For a resistive load and assuming that the internal impedance of the linear generator is predominately resistive, the current relations are derived simply by dividing by R, the net resistance of the stator coils plus the external load. Figure 7 is a graph of the voltage functions using some of the design parameters from the laboratory test device. Since all impedances are assumed to be resistive, plots of the current functions will yield the same plots.

Figure 8 is a pictorial representation of the mechanical forces acting on the stator pole faces and on the slidor center of mass. In addition to the force vectors in figure 8, one more force vectors is defined as the following:

$\underline{F}_{ex}$ = Resultant Electromagnetic Force along the x axis
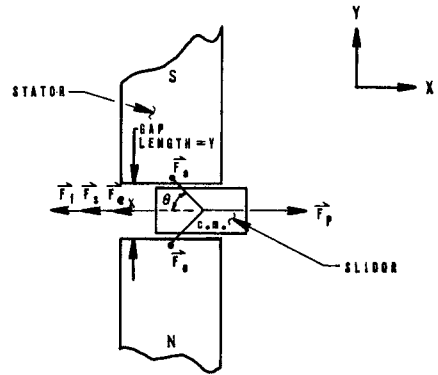
$\vec{F}_p = \underline{F}_p$ EXPLOSIVE PROPELLANT GENERATED FORCE (DRIVING FORCE)

$\vec{F}_e = \underline{F}_e$ ELECTROMAGNETIC FORCE

$\vec{F}_s = \underline{F}_s$ RESET SPRING FORCE

$\vec{F}_f = \underline{F}_f$ SMOOTH BORE AND SLIDOR FRICTION FORCE

Fig. 8. Electromechanical Forces

The idealized forces can be represented as acting on the center of mass of the permanent magnet structure of the slidor and at the center of the stator pole faces. The following relationship is derived from the figure.

$$\underline{F}_{net} = \underline{F}_p + 2\underline{F}_{ex} + \underline{F}_s + \underline{F}_f$$

where $\underline{F}_{ex} = -|\underline{F}_e| \cos(\Theta) \underline{k}_x$

From section 4, we have the expression for the kinetic energy released during the adiabatic expansion against the piston-slidor assembly.

$$Mu^2/2 = C\{\{[a(h+x)]^{1-\#} - [ah]^{1-\#}\}/(1-\#)\}$$

The work done by a force can be expressed by the following:

$$W = \int_{l1}^{l2} |\underline{F}| \cos(\Theta) ds$$

where (Θ) = the angle between the force vector and the direction of displacement.

For the case where the propellant generated force is parallel to the direction of motion, we have

$$W = \int_{x1}^{x2} |\underline{F}| dx.$$

By the First Theorem of Calculus we have

$$\underline{F} = (dW/dx) \underline{k}_x$$

where $\underline{k}_x$ is a unit direction vector, which leads to the relationship for the propellant force

$$\underline{F}_p = \{C/a\} (h + x)^{-\#} \underline{k}_x.$$

To determine the Electromagnetic Force $\underline{F}_e$, we use the following relationship.

$$Power = EMF^2/R$$

where R is the net electrical resistance of the stator coil and the load. Recalling that instantaneous power can be expressed as dW/dt we have the following

$$dW = (EMF^2/R) dt.$$

433

Since by definition,

$$W = \int_{x1}^{x2} |\underline{F}| \cos(\Theta)\, dx$$

we have the following expression for energy and the force, $\underline{F}_e$.

$$\cos(\Theta)|\underline{F}_e| = dW/dx$$

Note that $dW/dx = \{EMF^2/R\}(dt/dx)$ yields

$$\cos(\Theta)|\underline{F}_e| = \{EMF^2/R\}(1/u_2) \quad \text{where } u_2 = dx/dt.$$

Recall previously that

$$\underline{F}_{ex} = -|\underline{F}_e|\cos(\Theta)\,\underline{k}_x$$

then

$$\underline{F}_{ex} = -\{EMF^2/Ru_2\}\,\underline{k}_x.$$

For each phase of the slidor motion, $\underline{F}_{ex}$ will have a different form and hence so will $\underline{F}_{net}$. For the recoil or reset spring force we assumed a linear spring function.

$$\underline{F}_s = -Kx\,\underline{k}_x$$

where K = spring constant and the negative sign indicates that the spring is under compression.

Because lubricants were used liberally on the slidor and around the piston seals, we assumed that $\underline{F}_f$ = 0. Thus in general we have an the following expression for the net force.

$$\underline{F}_{net} = [\{C/a\}(h + x)^{-\#} - 2\{EMF^2/Ru_2\} - {}'Kx\,]\underline{k}_x.$$

For Phase I slidor motion, the second term of $\underline{F}_{net}$ becomes

$$2\{EMF^2/Ru_2\} = \{2/Ru_2\}[n1Bu_2 - \{n1BL/R\}(du_2/dt)]^2$$

and $\underline{F}_{net}$ becomes

$$\underline{F}_{net} = [(C/a)(h + x)^{-\#} - \{2(n1B)^2/R\}\{u_2 - (2L/R)(du_2/dt) + (L^2/R^2 u_2)(du_2/dt)^2\} - Kx]\,\underline{k}_x.$$

For Phase II slidor motion, the second term of $\underline{F}_{net}$ becomes

$$2\{EMF^2/Ru_2\} = \{2/Ru_2\}[n1Bu_2]$$

$$= (2n1B)/R$$

and $\underline{F}_{net}$ becomes

$$\underline{F}_{net} = [(C/a)(h + x)^{-\#} - (2n1B)/R - Kx]\,\underline{k}_x$$

$$= 0$$

For Phase III slidor motion, the second term of $\underline{F}_{net}$ becomes

$$2\{EMF^2/Ru_2\} = \{2/Ru_2\}[n1Bu_2 + \{n1BL/R\}(du_2/dt)]^2$$

and $\underline{F}_{net}$ becomes

$$\underline{F}_{net} = [(C/a)(h + x)^{-\#} - \{2(n1B)^2/R\}\{u_2 + (2L/R)(du_2/dt) + (L^2/R^2 u_2)(du_2/dt)^2\} - Kx]\,\underline{k}_x.$$

For Phase IV slidor motion, the previous equations repeat themselves except that $(C/a)(h + x)^{-\#}$ = 0 and the spring force term becomes positive. The general form for the net force then becomes

$$\underline{F}_{net} = [Kx - 2\{EMF^2/Ru_2\}]\,\underline{k}_x$$

Note that for Phases I, III, and IV slidor motion, the self-inductance terms dominate the equations for the net force. Also note that for the initial impulse of the slidor mechanical cycle, the only difference between the net force in Phase I motion and the net force in Phase III is the +/- sign after u_2 in the second term.
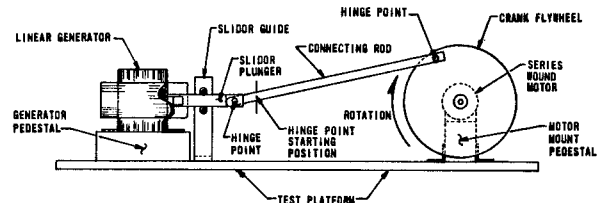
6. Linear Generator Tests

Fig. 9. Linear Generator Test Setup.

During the fall of 1984, the linear generator was tested using a motor driven flywheel and crank to drive the slidor back and forth in the stator (see figure 9). A variable sliding potentiometer was attached to the other end of the slidor to indicate position as it slid back and forth. The potentiometer is not shown in the figure. The total number of stator coil turns for this test was 68.
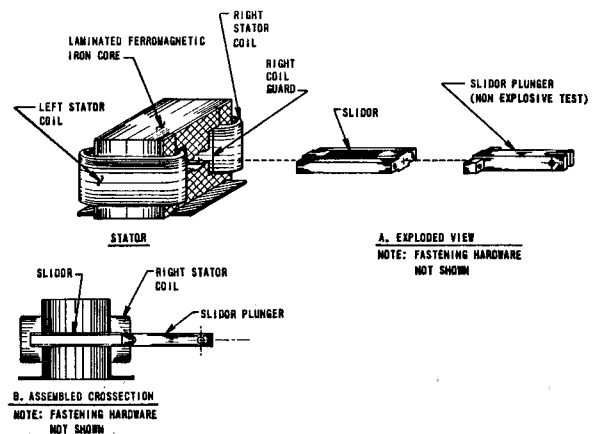

Fig. 10. Linear Generator Drawing.

Note that in figure 10 the stator coils are placed on the side of the ferromagnetic core instead of over the stator pole faces to minimize fringing effects and to facilitate study of the flux variations in the flux path as a function of slidor motion. A practical device for the production of usable power would have coils wrapped around the

stator pole faces to maximize coupling between the slidor magnetic field and the stator coils.
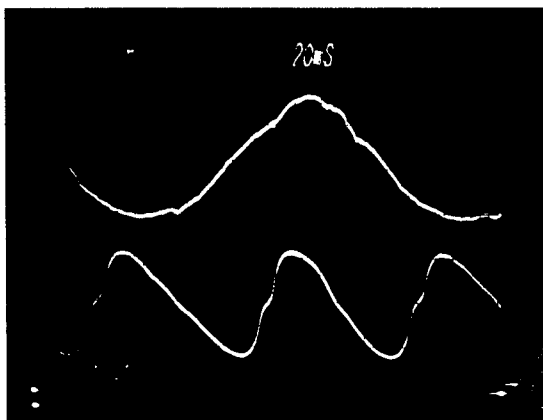

Fig. 11. Linear Generator Output Waveforms.

Figure 11 illustrates a typical oscilloscope graph from the dynamic testing of the linear generator on its flywheel test stand. The top line is a trace of the position of the slidor as a function of time. The first order derivative along this trace indicates the instantaneous velocity of the slidor. The bottom line is trace of the output voltage from the stator coils during motion of the slidor. The graticule line through the horizontal center of each waveform is the null position. With our present understanding, it appears that the doubling of the output voltage frequency in relation to the mechanical frequency of the slidor is caused by the self-inductance of the stator. Also, the stator self-inductance seems to be the cause for the saw-tooth appearance of the output voltage.

7. Recovery and Reset Design Considerations

If the electrical load is properly selected to match the explosive propellant load, there should be only enough kinetic energy remaining to reset the generator system to the start geometry. For a small scale device such as the laboratory proof-of-principle demonstrator, this energy could be stored in a reset spring with an associated pnuematic one-way viscous damper (see figure 12).
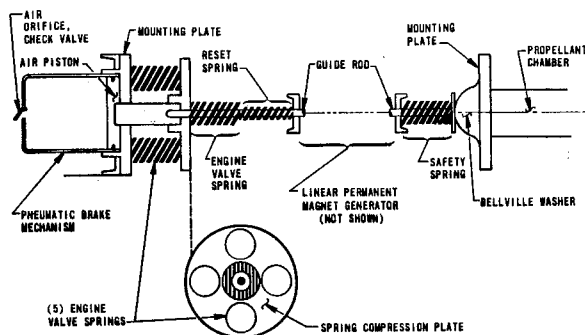

Fig. 12. Recover/Reset Mechanism Drawing.

The viscous damper would damp out mechanical oscillations of the piston-slidor assembly after the

electrical pulse is generated. For a high power device the reset mechanism would probably be a pneudraulic system similar to the "long-recoil cylinder" which is used in modern artillery pieces to reset the gun after firing (see figure 13).
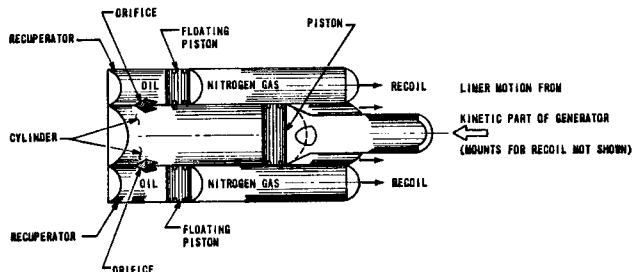

Fig. 13. "Long-recoil" Cylinder Drawing

8. Generator System Tests

During the fall of 1986 and into the spring of 1987, test firings were conducted at the AF Weapons laboratory to observe pulse generator performance at various propellant loads. For each cartridge fired oscilloscope graphs were recorded. As in the previous tests of the linear generator, the stator coils are on the side of the ferromagnetic core instead of over the stator pole faces.

The test firings were conducted at the Plasma Physics Branch of the Air Force Weapons Laboratory on three occasions: 20 Sep 1986, 2 Jan 1987, and 13 Apr 1987. The cartridges for the September test contained "factory load" powder with a wax plug. The January and April cases used Hercules "Unique" and DuPont IMR 4198 gunpowder, respectively. The generator was modified between tests to produce larger output pulses.

Three cartridges were fired during the September test. Each case contained 2 grains of Winchester Super X "factory load" propellant. The first two contained a "5-6 drops" wax plug, and the third contained a "3 drops" wax plug. The generator had 68 turns of 3 gauge 8 strand wire. The electrical load consisted of a 0.1 (ohm) resistor made from nichrome 1/8 inch flat wire. A Tektronix 549 oscilloscope with a camera and Polaroid 612 film was used to record the voltage across the load. The first two shots failed to trigger the oscilloscope, and the third produced a trace showing only noise from the generator's electromagnetic actuator. The noise appeared as a spike at the beginning of the trace.

After the September test, several modifications were made to the generator. The two forward safety springs (see figure 2) were replaced with a single spring, and the inner reset spring was replaced with a less stiff spring. The springs were replaced to give the generator slidor a free range of motion and hence larger output pulses.

The January test consisted of eleven shots with live cartridges. In each case, there was 1 to 5 grains of Hercules "Unique" double-base smokeless powder made from nitroglycerin and nitrocellulose mixed with other ingredients. Each case was sealed with about 3 drops of wax. As in the September test, the electrical load was 0.1 ohms. The voltage across the load was recorded with Tektronix 7603 oscilloscope with a camera and Polaroid 612 film. All of the oscillographs showed flat traces. A few had a noise spike at the beginning of the trace from the solenoid actuator.

We suspected three causes for the lack of an output pulse. First, that the generator barrel was blocked in front of the piston. This was confirmed

435

when the generator was taken apart after testing. The barrel was clogged with a 0.5 inch plug of wax and spent powder residue. The plug was removed, and the barrel was cleaned and lubricated.

The second cause appeared to be due to the type of gunpowder used. In pulsed systems theory, it is important to match the impulse response of a system to the impulse of the external driving force to assure optimum energy transfer between the system and the driving force. The Hercules powder is a fast burning mixture designed for pistol and small rifle use. The Lyman Loading Handbook[8] identifies it as suitable for the lighter bullet loads of the .22 Hornet. Whereas, DuPont IMR 4198 is a slow burning powder and was identified by the loader's manual as suitable for the heaviest loads of the .22 Hornet. Since the slidor mass is about 704 grams and the heaviest .22 Hornet bullet is about 3.6 grams, DuPont IMR 4198 smokeless powder was chosen for the next five tests to ensure some energy transfer between the propellant and the generator.

The generator system was originally designed to support 8 mm cases with a maximum load of up to 1.88 grams of propellant. Safety considerations forced derating the device to .22 caliber cases with a maximum powder load of .65 grams (10 grains) of propellant.

Finally, the third reason for the lack of an output signal was that the number of ampere turns in the generator coils were too low. The first set of coils were tested by striking the generator slidor with a rubber mallet and measuring the open load voltage with a Tektronix 310 oscilloscope. The open load signal was below the background noise level on the oscilloscope, so we replaced the generator coils. The original generator system had two 34 turn coils of 3 gauge 8 strand wire connected in series. These coils were replaced with two 450-turn coils of 18 gauge double strand transformer wire. The new coils were then tested with the rubber mallet. The coils produced an open load signal of 0.25-0.50 volts on a 5 millisecond per division sweep speed. The signals resembled a single triangular pulse.

Table 2

SELECTED SHOTS FROM THE APRIL TEST

SHOT No.	DRIVER	ELECTRICAL LOAD	PEAK VOLTAGE	PULSE WIDTH	PEAK POWER	TOTAL ENERGY DELIVERED
		(OHM)	(VOLTS)	(MILLISEC.)	(MILLIWATTS)	(JOULES)
1.	MANUAL	OPEN	0.82	20	---	---
2.	MANUAL	150	0.6	20	2.4	---
8.	POWDER	150	0.058	20	0.021	2.9×10^{-7}
9.	POWDER	150	0.084	20	0.045	5.3×10^{-7}
10.	POWDER	150	0.044	20	0.013	1.2×10^{-7}
11.	POWDER	OPEN	0.078	20	---	---
14.	POWDER	470	0.20	20	0.084	13.0×10^{-7}

The April test sequence consisted of three hand-driven shots, three solenoid driven shots, and eight case driven shots. Each case contained 9.5 grains of DuPont IMR 4198 smokeless powder, and was sealed with approximately 6 drops of wax. Three different electrical loads were tried: open circuit, 150 (ohm), and 470 (ohm). Higher resistances were used to produce a larger output voltage pulse. As before, the load voltage was recorded on a Tektronics 7603 oscilloscope with a camera and Polaroid 612 film. Results from selected shots are summarized in table 2.

We first tested the system by pushing the slider with our hands. The first two "shots" were conducted with an open load and produced peak signals of 0.40 and 0.82 volts, respectively. Figure 14 is a plot of the signal from the first shot. The first hand-driven shot was into the 150 (ohm) load (158.4 ohm measured) and produced a peak signal of 0.68 volts.
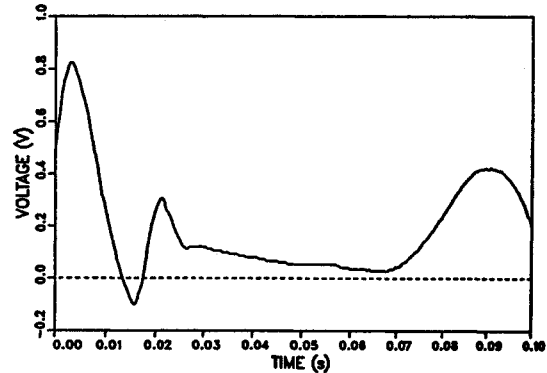
SHOT 1, HAND DRIVEN, OPEN LOAD

Fig. 14. Hand Driven Shot.

The next three shots were taken to record the noise from the solenoid driver. We fired the solenoid actuator with no propellant charges or cases in the breech but with a 150 ohm electrical load connected to the linear generator's output terminals. Two shots produced flat traces, and the third failed to trigger the oscilloscope.
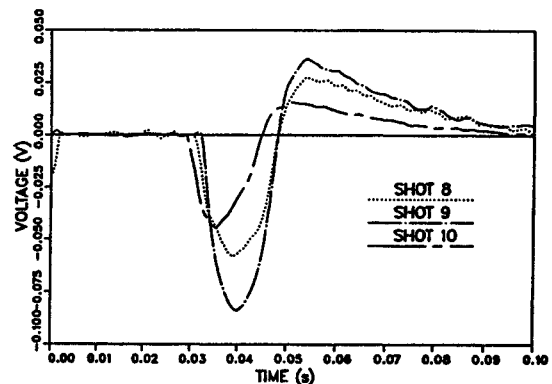
POWDER DRIVEN, 150 OHM LOAD

Fig. 15.

The remaining shots were driven by the powder cases. Figure 15 shows the voltage traces from the three shots into the 150 ohm load. The peak signals were 0.044, 0.058, and 0.084 volts. The shape of the signals were the same. The first pulse is due to the forward motion of the slider, and the backswing is due to the reset motion of the recoil spring. The variation in signals is due to slightly different cases and to buildup of debris in the generator barrel. The best 150 ohm shot produced 0.084 volts, 4.5×10^{-5} watts of power, and delivered 5.3×10^{-7} joules of energy to the load.

Figures 16 and 17 show the voltage signals from an open load and 470 ohm (460.8 measured) load. The open load peak voltage was 0.078 volts, and the 470 ohm load peak signal was 0.20 volts. The generator was lubricated just prior to the 470 ohm shot,

436

resulting in the highest output voltage. The 470 ohm shot was the best shot to date, producing 0.20 volts, 8.4×10^{-5} watts of power, and delivering 1.3×10^{-6} joules of energy to the load.
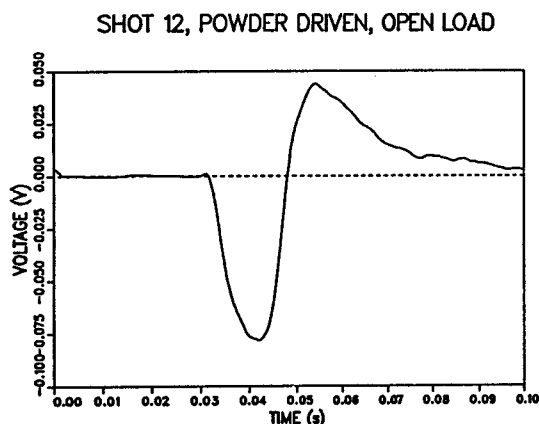
SHOT 12, POWDER DRIVEN, OPEN LOAD

Fig. 16.

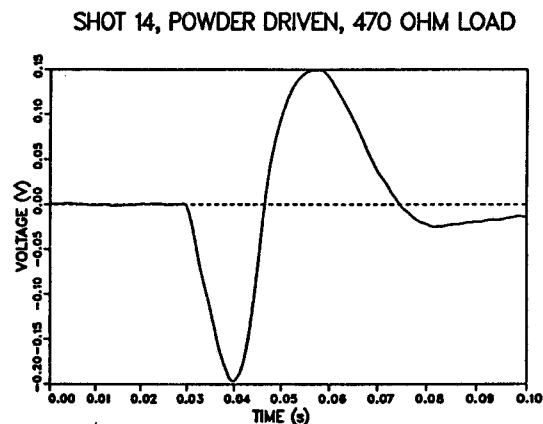SHOT 14, POWDER DRIVEN, 470 OHM LOAD

fig. 17.

9. Summary

This device has several potential advantages over prior techniques for generating pulsed high power. Except for high explosive driven pulse generators, it potentially has the highest power density of any known pulsed high power device. Once the propellant is burned, the device is off, thereby eliminating the need for elaborate switching techniques to turn the power off. Initiation of the propellant turns the device on. The quantity of energy per pulse can be quantized by selecting the appropriate propellant load per case. To minimize debris buildup in the expansion chamber, caseless cartridges could be used. Generator geometry and coil design can be selected beforehand to match the generator's impedance to the load impedance. Finally, with the appropriate automatic case feed mechanism, it can be designed to generate power pulses at a rate of up to 60 pulses per second (pps).

10. References

[1] R. L. Schlicher, "Repeatable Explosive-Driven Pulse Generator System and Method," U. S. Patent 4,594,521, U. S. Patent Office, 1986.

[2] R. S. Caird, C. M. Fowler, D. J. Erickson, B. L. Freeman, W. B. Garn, "Survey of Recent Work on Explosive Driven Magnetic Flux Compression Generators," International Conference on Energy Storage, Compression and Switching, Venice, Italy, 1978.

[3] C. B. Gardner, "Projectile-Actuated Surge Generator," U. S. Patent 2,544,077, U. S. Patent Office, 1948.

[4] S. D. Weisman, "Firearm Activated Generator," U. S. Patent 3,257,905, U. S. Patent Office, 1966.

[5] F. W. Sears and M. W. Zemansky, University Physics, 3rd ed., Addison-Wesley, Reading, MA, 1964.

[6] P. Lorrain and D. Corson, Electromagnetic Fields and Waves, 2nd ed., W. H. Freeman and Co., San Francisco, 1970.

[7] Hitachi Magnetics Corp., Permanent Magnet Manual Edmore, Michigan, 1975.

[8] J. Sheridan, ed., Lyman Reloading Handbook, 45th ed., Lyman Products Corp., 1970.